COMPACT POLARIMETRY IN A LOW FREQUENCY SPACEBORNE CONTEXT

M-L. TRUONG-LOÏ[1], A. FREEMAN[1], P. DUBOIS-FERNANDEZ[2], E. POTTIER[3]

1. Jet Propulsion Laboratory, California Institute of Technology, 4800 Oak Grove Drive, Pasadena, CA 91109, USA, my-linh.truong-loi@jpl.nasa.gov, +1-818-354-1206
2. ONERA, BA 701, 13661 Salon de Provence, AIR CEDEX, France
3. IETR, UMR CNRS 6164, Université Rennes1, 263 Avenue Général Leclerc, 35000 Rennes, France

1. INTRODUCTION

Compact polarimetry has been shown to be an interesting alternative mode to full polarimetry when global coverage and revisit time are key issues [1-4]. It consists on transmitting a single polarization, while receiving on two. Several critical points have been identified, one being the Faraday rotation (FR) correction and the other the calibration. When a low frequency electromagnetic wave travels through the ionosphere, it undergoes a rotation of the polarization plane about the radar line of sight for a linearly polarized wave, and a simple phase shift for a circularly polarized wave. In a low frequency radar, the only possible choice of the transmit polarization is the circular one, in order to guaranty that the scattering element on the ground is illuminated with a constant polarization independently of the ionosphere state. This will allow meaningful time series analysis, interferometry as long as the Faraday rotation effect is corrected for the return path. In full-polarimetric (FP) mode, two techniques allow to estimate the FR: Freeman method using linearly polarized data [5-6], and Bickel and Bates theory based on the transformation of the measured scattering matrix to a circular basis [7]. In CP mode, an alternate procedure is presented which relies on the bare surface scattering properties. These bare surfaces are selected by the conformity coefficient [4], invariant with FR. This coefficient is compared to other published classifications to show its potential in distinguishing three different scattering types: surface, double-bounce and volume. The performances of the bare surfaces selection and FR estimation are evaluated on PALSAR and airborne data. Once the bare surfaces are selected and Faraday angle estimated over them, the correction can be applied over the whole scene. The algorithm is compared with both FP techniques. In the last part of the paper, the calibration of a CP system from the point of view of classical matrix transformation methods in polarimetry is proposed.

2. WAVE PROPAGATION IN THE IONOSPHERE LAYER

The ionosphere is a part of the upper atmosphere comprising three neutral layers: the mesosphere, the thermosphere and the exosphere. It is ionised by solar radiation and its layers are determined by the electrons and positives ions density. Free electrons interact with a wave propagating in the ionosphere by modifying its characteristics, i.e. polarization, amplitude, phase, etc. Ionosphere importance comes from its significant influence on lower frequencies. Effects resulting from the wave propagation in the ionosphere are : phase advance of the wave compared to propagation in the vacuum, group delay, ionospheric scintillations and Faraday rotation [8]. The latter phenomenon is linked to the influence of the Earth magnetic field on the electrons motion. The medium is birefringent, so a linearly polarized incident wave is divided into two circularly polarized waves, left and right, from the beginning of the propagation in the ionosphere. The propagation speed of these two waves being not equal, the propagation plane of the linearly polarized wave reconstructed at the output of the ionosphere is different from the incident one. The angle difference between both planes is called the Faraday rotation and can be computed by the following expression:

$$\Omega = \frac{K}{f^2} B \cos\eta \sec\phi . (TEC) \tag{2.1}$$

Where Ω is the Faraday angle, B is the Earth magnetic field intensity, K is a constant, f is the radar frequency, ϕ is the incidence angle and η is the angle between the radar line of sight and the Earth magnetic field. Smaller is the radar frequency, bigger is the Faraday rotation. Phase advance, group delay and scintillations do not have any interest in compact polarimetry, so in this paper, we are focusing on Faraday rotation.

Bickel and Bates showed that it is possible to compute the Faraday rotation from both cross-polarized waves in a circular basis [7]. Using L-band linearly polarized backscatters measurements, Freeman showed that for a small angle, i.e. Ω smaller than 45°, the Faraday rotation angle can be detected by a 180° phase change in the computation of $\left\langle M_{HV} M_{VH}^{*} \right\rangle$ phase argument, where *M* stands for *measured* scattering elements [5]. Then, to estimate the Faraday

rotation angle, Freeman introduced a method based on averaged second order statistics and assuming no reciprocity in the cross-polarized measurements. Using $Z_{HV} = \frac{1}{2}\left(M_{HV} - M_{VH}\right)$, Freeman computes the Faraday rotation with the following equation [6]:

$$\Omega = -\frac{1}{4}\arg\left(Z_{HV} Z_{VH}^{*}\right) \tag{2.2}$$

To correct for the Faraday rotation, i.e. to retrieve the Sinclair matrix *S*, the following matrix multiplication has to be done:

$$S = R_{\Omega}^{T} M R_{\Omega}^{T} \tag{2.3}$$

Where R_{Ω} is the Faraday rotation matrix equal to: $R_{\Omega} = \begin{pmatrix} \cos\Omega & \sin\Omega \\ -\sin\Omega & \cos\Omega \end{pmatrix}$ and $R_{\Omega}^{T} \equiv R_{\Omega}^{-1}$. This estimate is known modulo π/2.

In compact polarimetry, the Faraday rotation affects only the polarisation in reception since the transmission is circularly polarized. In the π/2 context with a right circularly polarized wave in transmission and two linearly polarized waves in reception, the backscattering vector is expressed by the following expression:

$$\begin{pmatrix} k_1 \\ k_2 \end{pmatrix} = \frac{1}{\sqrt{2}} \begin{pmatrix} \cos & \sin\Omega \\ -\sin\Omega & \cos\Omega \end{pmatrix} \begin{pmatrix} S_{HH} & S_{HV} \\ S_{VH} & S_{VV} \end{pmatrix} \begin{pmatrix} \cos & \sin\Omega \\ -\sin\Omega & \cos\Omega \end{pmatrix} \begin{pmatrix} 1 \\ -j \end{pmatrix} \tag{2.4}$$

The three possible computations in the π/2 context, i.e. $\left\langle M_{RH} M_{RH}^{*} \right\rangle$, $\left\langle M_{RV} M_{RV}^{*} \right\rangle$ and $\left\langle M_{RH} M_{RV}^{*} \right\rangle$, are not sufficient to estimate the Faraday rotation. Bare surface backscattering properties allow to simplify these expressions and lead to an estimate of the Faraday rotation.

3. SELECTING BARE SURFACES

The selection of bare surfaces from CP data can be achieved based on the conformity coefficient which has been shown to be invariant with Faraday rotation [4]. This coefficient, used in CP mode as well as FP mode, allows discriminating the three main scattering types (surface, double-bounce and volume scattering) and is expressed as:

$$\mu = \frac{2\Im\left\langle M_{RH} M_{RV}^{*} \right\rangle}{\left\langle M_{RH} M_{RH}^{*} \right\rangle + \left\langle M_{RV} M_{RV}^{*} \right\rangle} = \frac{2\Im\left\langle S_{RH} S_{RV}^{*} \right\rangle}{\left\langle S_{RH} S_{RH}^{*} \right\rangle + \left\langle S_{RV} S_{RV}^{*} \right\rangle} \tag{3.1}$$

$$\mu = 2\frac{\Re\left(S_{HH} S_{VV}^{*}\right) - \left|S_{HV}\right|^{2}}{\left(\left|S_{HH}\right|^{2} + 2\left|S_{HV}\right|^{2} + \left|S_{VV}\right|^{2}\right)} \tag{3.2}$$

where M_{RH} and M_{RV} are the measured scattering elements, considering a right circular transmission and two linear receptions (H & V), subject to Faraday rotation. S_{RH} and S_{RV} are the measured scattering elements, considering a right circular transmission and two linear receptions assuming Faraday rotation corrected or missing. S_{HH}, S_{HV} and S_{VV} are Sinclair matrix terms without Faraday effect.

We notice that both expressions of μ in (3.1) are equal insuring the FR invariance of the conformity coefficient. Then, assuming reflection symmetry, this classification can be written in FP mode, cf. (3.2).

When $t_1<\mu<1$ the scattering element is identified as a surface, $t_2<\mu<t_1$ identified a volume and $-1<\mu<t_2$ describes a double-bounce scattering.

This scattering characterization is evaluated against the output of the Cloude-Pottier [9] and Freeman-Durden [10] classifications over RAMSES data as shown in Fig.1(a).

It is noted in Fig. 1(a) that most fields that are identified as surfaces with the Cloude-Pottier and the Freeman-Durden decompositions are also identified as surfaces with the conformity coefficient (in blue).

The thresholds values were adjusted over several scenes of different types. In Fig.1(b), values of μ are displayed over each scattering types selected by Cloude-Pottier classification. Each of the curves corresponds to one class identified by the Cloude-Pottier classification, i.e. surface in blue, volume in green and double-bounce scattering in red. It represents the histogram of the μ coefficient in this particular class. This plot confirms the overall agreement between the two classifiers.

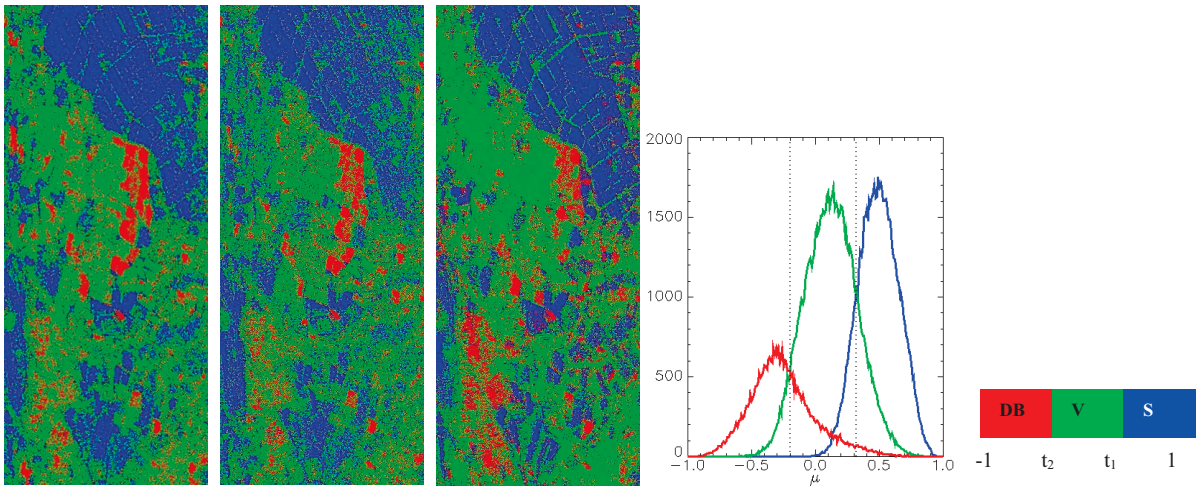

(a) (b)

Fig. 1 : (a) on the left hand side is displayed the Cloude-Pottier classification. In the middle, the conformity coefficient is estimated, then on the right hand side the Freeman-Durden classification is shown. (b) Three plots displaying the values of μ depending on the scattering type. In blue, the values of μ for a surface, in green for volume and in red for a double-bounce. The scattering type has been selected by the Cloude-Pottier classification.

The thresholds are chosen at the curves intersection : t_1=0.35 and t_2=-0.2. However, note that these thresholds are dependent of the imaged scene and they are not definitely set. Nevertheless, they are confirmed by confusion matrices computed between μ and Cloude-Pottier on one hand and μ and Freeman-Durden on the other hand, cf. (3.3).

$$\begin{array}{cc} & H/\alpha \\ & \begin{array}{ccc} S & V & DB \end{array} \\ \begin{array}{c} \\ S \\ \mu\ V \\ DB \end{array} & \begin{bmatrix} 30.31 & 6.23 & 0.44 \\ 6.66 & 36.26 & 2.06 \\ 0.04 & 6.54 & 11.46 \end{bmatrix} \end{array} \qquad \begin{array}{cc} & FD \\ & \begin{array}{ccc} S & V & DB \end{array} \\ \begin{array}{c} \\ S \\ \mu\ V \\ DB \end{array} & \begin{bmatrix} 22.78 & 14.18 & 0.02 \\ 9.70 & 29.75 & 9.59 \\ 0.01 & 5.45 & 8.52 \end{bmatrix} \end{array} \tag{3.3}$$

4. FARADAY ROTATION ESTIMATE

Once the bare surfaces are selected, the Faraday rotation can be estimated over them as shown in the following. To estimate the Faraday rotation, we rely on two assumptions based on natural surfaces properties. The first assumption is the reflection symmetry, valid over surfaces presenting symmetry with respect to the vertical plane containing the line of sight. In that case, it can be shown that the averaged cross products between the co- and cross-pol channels are equal to zero:

$$\left\langle S_{HH} S_{HV}^* \right\rangle \approx \left\langle S_{VV} S_{HV}^* \right\rangle \approx 0 \tag{4.1}$$

The second hypothesis assumes that the phase between the co-pol channels is close to zero for bare surfaces:

$$Arg\left\langle S_{HH} S_{VV}^* \right\rangle \approx 0 \tag{4.2}$$

Providing these two assumptions, we can then estimate the Faraday rotation angle with one of these following equations:

$$\Omega = \frac{1}{2} Arg\left\langle M_{RR} M_{RL}^* \right\rangle \pm n\frac{\pi}{2} \tag{4.3}$$

$$\Omega = \frac{1}{2} Arc\tan\left(2\frac{\mathrm{Re}\left(M_{RH} M_{RV}^*\right)}{\left(\left\langle M_{RV} M_{RV}^* \right\rangle - \left\langle M_{RH} M_{RH}^* \right\rangle\right)} \right) \pm n\frac{\pi}{4} \tag{4.4}$$

$$Arg\left\langle \widetilde{S}_{Rh} \widetilde{S}_{Rv}^* \right\rangle = 90° \pm n\pi \tag{4.5}$$

Where $\widetilde{S}$ is the corrected data over all possible values of FR from 0° to 180°.

The estimations of the Faraday rotation associated with these three equations are compared to the Faraday angle estimation provided by Bickel and Bates in one part and by Freeman in another part. Fig. 2 shows that the estimations using CP data are in agreement with the estimations using FP data and correct, despite the fact that it is more precise with FP data. So FR estimate is possible directly with CP data. Note that the third technique relying on (4.5) provides an estimate modulo π.

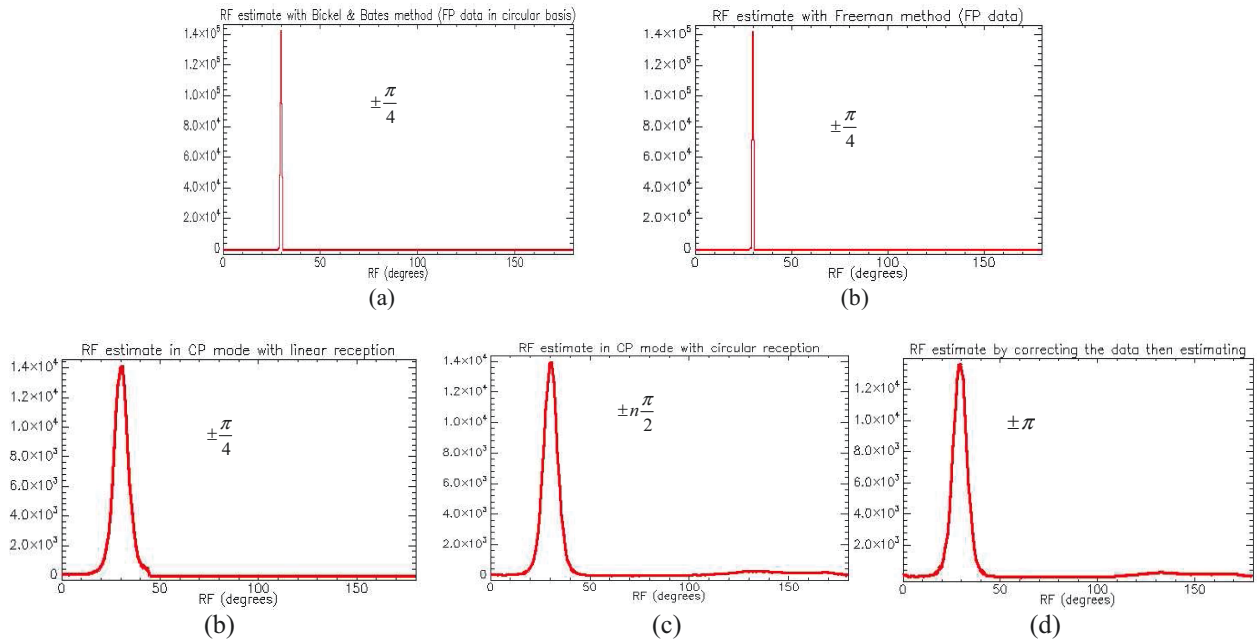

Fig. 2 : FR over PALSAR data. A FR of 30° has been introduced in FP data (a,b) and in synthesized CP data (c,d,e). (a) Bickel and Bates, (b) Freeman, using FP data over the whole scene. (c,d,e) CP methods are tested over bare surfaces previously selected by the conformity coefficient. (c) estimation using Eq. (4.4), (d) using Eq. (4.3), (e) using Eq. (4.5).

5. COMPACT-POL CALIBRATION

In a full-polarimetric context, ignoring the system gain function and noise, the calibration is done based on external targets like a trihedral and distributed targets enforcing the reciprocity principle. Once the distortions, i.e. channel imbalance and cross-talk, are estimated, it is possible to correct the system (i.e. to retrieve the Sinclair matrix elements) by computing an inversion matrix. In the π/2 context with a circular transmission, it has been shown that it is not possible to correct the transmission afterwards as only one polarization is transmitted [11] and it is illustrated in the diagram at the bottom of this page. So considering now that the system is almost perfect in transmission, 5 distortion parameters need to be corrected. We suggest a procedure to calibrate such a system using three external targets. Two dihedrals at 0° (noted D^0) and 45° (noted D) and a trihedral (noted T) are necessary to correct for channel imbalance, cross-talk, FR and system gain. Note that in FP, only one trihedral is needed to calibrate the system because of enforcing the reciprocity principle (HV=VH). Even if in CP fewer calibration unknowns need to be estimated, more external targets are required to calibrate the system.

$$\begin{pmatrix} M_{RH} \\ M_{RV} \end{pmatrix} = A(r,\theta)e^{j\varphi}\frac{1}{\sqrt{2}}\begin{pmatrix} 1 & \delta_2 \\ \delta_1 & f_1 \end{pmatrix}\begin{pmatrix} \cos\Omega & \sin\Omega \\ -\sin\Omega & \cos\Omega \end{pmatrix}\begin{pmatrix} S_{hh} & S_{hv} \\ S_{vh} & S_{vv} \end{pmatrix}\begin{pmatrix} \cos\Omega & \sin\Omega \\ -\sin\Omega & \cos\Omega \end{pmatrix}\boxed{\begin{pmatrix} 1 & \delta_3 \\ \delta_3 & f_2 \end{pmatrix}\begin{pmatrix} 1 \\ -j \end{pmatrix}}$$

$$\alpha\begin{pmatrix} 1 \\ -j \end{pmatrix} + \beta\begin{pmatrix} 1 \\ j \end{pmatrix}$$

$$\alpha = \frac{1+f_2}{2} \qquad \beta = \frac{1-f_2}{2} - j\delta_3$$

$$\alpha \sim 1 \qquad \beta \sim -j\delta$$

$f_2 \sim 1$

Results for the four different unknowns are the following:

$$\delta_1 = \frac{j}{2}\left(\frac{M^{*D^0}_{RV}}{M^{D^0}_{RH}} \frac{M^{D}_{RV}}{M^{D}_{RH}} - \frac{M^{D}_{RH}}{M^{D}_{RV}} \frac{M^{D^0}_{RV}}{M^{D^0}_{RH}} \right) \tag{5.1}$$

$$f_1 = \frac{2j}{\frac{M^{T}_{RH}}{M^{T}_{RV}} - \frac{M^{D}_{RH}}{M^{D}_{RV}}} \tag{5.2}$$

$$\delta_2 = |f_1|^2 \frac{M^{D^*}_{RH}}{M^{D^*}_{RV}} - \delta_1^* f_1 - jf_1 \tag{5.3}$$

$$\delta_2 = |f_1|^2 \frac{M^{D^*}_{RH}}{M^{D^*}_{RV}} - \delta_1^* f_1 - jf_1 \tag{5.4}$$

Note that the orientation of the dihedral, compared to the horizontal plane, known as hard to carry out, introduces only a phase delay in the compact-pol π/2 context. However the orientation compared to the perpendicular plane of the radar line of sight is difficult to realize.

Other directs methods could be assessed. First of all, the response from a trihedral corner reflector in H and V polarizations should have the same amplitude but a relative phase of 90° (and opposite sense compared to the transmitted one). If imbalances appear in the receptions channels, these differences can be directly observed, measured and converted to calibration coefficients. Then, another method is the one proposed by McKerracher for the calibration of the two dual-pol mini-RF SAR that observes the moon. This approach uses the response from the nadir which is similar to a quasi-specular reflection for which H and V polarizations are equivalent [12].

6. CONCLUSION

In presence of FR, the choice of the transmit polarization is important. Indeed, we have seen that at low frequency, circularly polarized wave in transmission is the only solution to overcome FR effect, as the EM wave seen by the scattering element has a constant polarization whatever the FR. On receive, the Faraday rotation can be corrected for if known. An estimation technique is presented based on the bare surface properties. The selection of the bare surfaces can be done using the conformity coefficient, itself Faraday rotation invariant.

Finally, a method allowing the calibration of a compact-pol system including the Faraday rotation effect using corner reflectors, a trihedral and two dihedral oriented at 0° and 45°, and assuming a perfect transmission is presented. Other direct methods using only a trihedral or the response from the nadir as McKerracher proposed for the calibration of the two dual-pol mini-RF SAR that observes the moon can be used.

7. ACKNOWLEDGMENT

The authors would like to thank their colleagues from the French Aerospace Lab (ONERA) for providing the RAMSES data.The research was conducted under a grant by CNES and ONERA. Part of this work was carried out at the Jet Propulsion Laboratory, California Institute of Technology, under contract to the National Aeronautics and Space Administration.

8. REFERENCES

[1] J-C. Souyris, P. Imbo, R. FjØrtoft, S. Mingot and J-S Lee, "Compact Polarimetry Based on Symmetry Properties of Geophysical Media : The $\pi/4$ Mode", IEEE Trans. Geosci. Remote Sens., vol. 43, no. 3, pp. 634-646, Mar. 2005.

[2] P.C. Dubois-Fernandez, J-C. Souyris, S. Angelliaume and F. Garestier, "The Compact Polarimetry for Spaceborne SAR at Low Frequency", IEEE Trans. Geosci. Remote Sens., vol. 46, no. 10, Oct. 2008.

[3] R. K. Raney, "Hybrid-Polarity SAR Architecture", IEEE Trans. Geosci. Remote Sens., vol. 45, no. 11, pp. 3397-3404, Nov. 2007.

[4] M-L. Truong-Loï, A. Freeman, P. Dubois-Fernandez and E. Pottier, "Estimation of Soil Moisture and Faraday Rotation From Bare Surfaces Using Compact Polarimetry", IEEE . Geosci. Remote Sens., vol. 47, no. 11, pp. 3608-3615, Nov. 2009.

[5] A. Freeman, and S. Saatchi, "On the Detection of Faraday Rotation in Linearly Polarized L-Band SAR Backscatter Signatures", Trans. On Geoscience and Remote Sensing, vol. 42, No. 8, pp. 1607–1616, 2004.

[6] A. Freeman, “Calibration of Linearly Polarized Polarimetric SAR Data Subject to Faraday Rotation”, IEEE Transactions on Geoscience and Remote Sensing, vol. 42, no. 8, pp. 1617-1624, Août 2004.
[7] S. H. Bickel and R. H. T. Bates, “Effects of magneto-ionic propagation on the polarization scattering matrix”, Proc. IRE, vol. 53, pp. 1089–1091, 1965.
[8] L. Castanet, P. Lassudrie-Duchesne, “Propagation des ondes radioélectriques à travers l’atmosphère”, Techniques de L’Ingénieur, REF. E1163, 10 mai 2008.
[9] S.R. Cloude and E. Pottier, “An Entropy Based Classification Scheme for Land Applications of Polarimetric SAR”, IEEE Transactions on Geoscience and Remote Sensing, vol. 35, no. 1, pp. 68-78, January 1997.
[10] A. Freeman and S. L. Durden, “A Three-Component Scattering Model for Polarimetric SAR Data”, IEEE Transactions on Geoscience and Remote Sensing, vol. 36, no. 3, pp. 963-973, May 1998.
[11] A. Freeman, P. Dubois-Fernandez and M-L. Truong-Loï, “Compact Polarimetry at Longer Wavelengths – Calibration”, Proceedings EuSAR 2008, Friedrichshafen, Germany, June 2008.
[12] P.L. McKerracher, J.R. Jensen, H.B. Sequeira, R.K. Raney, R.C. Schulze, D.B.J. Bussey, B.J. Butler, C.D. Neish, M. Palsetia, G.W. Patterson, P.D. Spudis, B.J. Thomson, F.S. Turner, “Mini-RF Calibration, a Unique Approach to On-Orbit Synthetic Aperture Radar System Calibration”, 41st Lunar and Planetary Science Conference, 2010.